Reconfiguration Algorithm to Reduce Power Losses in Offshore HVDC Transmission Lines

Inés Sanz, Miguel Moranchel, Javier Moriano, *Student Member, IEEE*, Francisco Javier Rodríguez, *Member, IEEE*, and Susel Fernández

***Abstract*—The race to increase the efficiency and reduce the power losses in transmission systems has resulted in the substantial growth of high-voltage direct current (HVDC) transmission systems. Moreover, the interconnection of these transmission systems significantly increases their reliability. However, the control of these meshed grids is a key problem that usually is managed through the control of the VSCs in those grids, but the control of the VSC can be complemented with a reconfiguration algorithm. This paper proposes the use of the particle swarm optimization algorithm, in order to reconfigure meshed HVDC transmission systems and reduce losses. The proposed algorithm has been tested in the CIGRE benchmark grid, which comprises of several offshore wind farms that generate energy sent to the grid through several HVDC transmission lines. The results show that as the energy generation changes due to wind changes, the grid topology must be reconfigured in order to achieve the maximum efficiency. Doing this reconfiguration, power savings around 18–19% could be achieved.**

***Index Terms*—High-voltage direct current (HVDC), off-shore, particle swarm optimization, reconfiguration, wind farm.**

I. Introduction

ENERGY consumption in the world is constantly growing [1], [2]. Simultaneously, environmental crisis caused by climate change should be mitigated. One way to reconcile these two facts is by using sustainable and clean energy sources, with high growth potential [3], [4]. Moreover, the electricity production cost from coal, gas, nuclear plants, and petroleum keeps rising, while the cost of renewable energy is clearly decreasing. For example, grid parity has already been achieved in many places, such as Hawaii [5].

Consequently, in the recent years, most countries have invested to improve the use of renewable energy, basically, solar photovoltaic, hydroelectric power, and wind energy. The main disadvantage of photovoltaic energy is the need for large tracts of lands to cover the demands of little urban zones, due to solar panels' low efficiency. Concentrating on hydroelectric power, this kind of energy is not available in all countries, like the Middle Eastern countries, and it is limited to very specific places. Moreover, this technology has several disadvantages that are related to environment, which diminishes people's interest in it. In contrast, wind energy uses a less amount of land to produce the same amount of energy. Nevertheless, wind energy has a great environment impact [1].

The energy produced by wind turbines is highly unpredictable due to multiple reasons, like wind behavior. To attenuate this variability, wind farms are being moved to the sea, where the wind regime is more consistent, and it is possible to occupy larger areas. In Northern Europe, there are many large offshore wind farms with power levels between 100 MW and up to gigawatts [7].

The transmission of all this energy from the sea to the land is a big challenge that has to be faced. High-voltage direct current (HVDC) grids are some of the best choices to connect this type of renewable source from the sea to the land [8], [9].

With technological advancement seen in semiconductors, HVDC transmission acquired importance, because it was becoming easier rise the voltage to unsuspected limits. Nowadays there are HVDC lines up to 800 kV, also called ultra-high voltage direct current (UHVDC) [10]. These types of lines are used when the amount of energy to be transmitted is very high.

In order to increase the reliability of the transmission and minimize the losses, multiterminal links are increasingly used to transmit energy from the farms to the land [11], [12]. Multiterminal links connect several wind farms together with several grids in the land. This produces a meshed transmission grid that allows the distribution of energy between different nodes.

The multiterminal VSC-HVDC system can connect different offshore substations with similar voltages. In the case of the stations with different voltages, it is possible the use of intermediate stations that implement a dc—ac–dc voltage transformation, in order to change the dc voltage as desired, although it is not essential [13].

The development of this type of connections requires proper high-level control methods [14]. The most-used control technique is the dc voltage-current droop control, which facilitates power flow control [15]. In this case, a reconfiguration algorithm could be used to control the multiterminal grid. In [16], a cooperative control based on droop control is proposed to maintain

Manuscript received June 17, 2016; revised November 17, 2016 and April 7, 2017; accepted May 16, 2017. Date of publication May 26, 2017; date of current version January 3, 2018. This work has been supported in part by research projects CONPOSITE (ENE2014-57760-C2-2-R Ministerio de Economía y Competitividad) and in part by PRICAM (S2013/ICE-2933 Consejería de Educación, Juventud y Deporte de la Comunidad de Madrid). This paper was presented at the International Conference on Renewable Energy Research and Application, Oct. 19–22, 2014, Milwaukee, WI USA. Recommended for publication by Associate Editor B. Singh. *(Corresponding author: Inés Sanz).*

The authors are with the Electronics Department, Universidad de Alcalá, Alcalá de Henares, Madrid 28801, Spain (e-mail: ines.sanz@depeca.uah.es; miguel.moranchel@depeca.uah.es; javier.moriano@depeca.uah.es; fjrs@depeca.uah.es; susel.fernandez@depeca.uah.es).

Color versions of one or more of the figures in this paper are available online at http://ieeexplore.ieee.org.

Digital Object Identifier 10.1109/TPEL.2017.2709259

the constant of the dc voltage. Other examples of control techniques for the reduction of losses can be found in [17]–[19].

Reconfiguration algorithms can change the interconnection between nodes according to specific requirements in order to achieve the best grid configuration. Reconfiguration can be ultimately considered to be a discrete nonlinear optimization problem, so, there are some optimization algorithms that can be used to solve this problem: The Ant Colony Optimization (ACO), the PSO, the evolutionary algorithms, the genetic algorithms, the fuzzy control, etc. In technical literature, there are some examples of optimization algorithms applied to the reconfiguration of ac grids. For example, in [20] and [21] ACO algorithm is used. This optimization method mimics the pheromone trail following the behavior of ants, where each ant perceives pheromone concentrations in its local environment and selects the direction with the highest pheromone concentration. From this principle, the best alternative (shortest path) from a collection of alternatives is found.

Evolutionary algorithms and genetic algorithms are two similar variants of the evolutionary computation, which has as its objective to mimic the processes from natural evolution. Some examples of these algorithms can be found in [22]–[28]. Basically, in these algorithms, the possible distribution grid configurations are represented through a population of chromosomes, and on that population are applied reproduction, crossover, mutation, and selection functions, in order to achieve the optimal chromosome that represents the best grid configuration.

The fuzzy control techniques can also be used to solve the reconfiguration problem. In [29], these kinds of techniques are used to deal with the reconfiguration of a grid with some distributed generation resources.

Particle Swarm Optimization algorithm has been used to solve the grid reconfiguration problem in [30] and [31]. For example, in [30] a distribution system reconfiguration methodology is developed, considering the reliability and power loss. In [31], a PSO algorithm is used to solve the optimal operation problem for the purpose of distribution reconfiguration, while considering the distributed generators. However, none of the studies mentioned above have analyzed the reconfiguration in the HVDC scenario.

In this paper, PSO algorithm is used to reconfigure the interconnection between the wind farms and the grids in the land over HVDC links, attending to minimize the transmission power losses.

The test grid presented in this paper is a modified system that is based on the test grid proposed in [32], which has been widely used to test control algorithms [33]–[35].

The paper is organized as follows. In Section II, the Particle Swarm Optimization algorithm used in this paper as the reconfiguration algorithm is explained. Section III contains a detailed description of the grid, as well as the generation profiles that are used to simulate different generation scenarios. Section IV summarizes the simulation results that are obtained by using the reconfiguration algorithm in the HVDC test grid. Finally, Section V includes the conclusions, and the references appear in Section VI.

II. PSO Reconfiguration Algorithm

PSO algorithm is proposed in this paper in order to minimize the power loss in the power transmission system, changing the interconnection between nodes.

In this algorithm, a group of particles move around the space of possible solutions, in which, each position represents a candidate solution to the reconfiguration problem. Each particle moves through the search space, adjusting its position according to its own experience and also to the neighboring particles experience. Its movement will be also influenced by its previous trajectory, what means, there is an inertia component in the particle movement. Therefore, a particle uses the best position found by itself, and the best position of its neighbors as well, to locate itself toward an optimal solution, the same manner as birds in a flock. The suitability of each particle is measured according to a fitness function that, in this case, depends on the power loss of the transmission system.

In the reconfiguration problem, the possible positions for the particles are vectors, which represent the possible status combinations of the switches in the power transmission system. Thus, each position vector is a binary vector, whose elements represent the states of the switches: "1" for the close state, and "0" for the open state. Therefore, position vectors have as many elements as switches in the system. To find the optimal solution of the reconfiguration problem, several particles are employed. In this case, the chosen number of particles is: $100 *$ number of switches, such as in [30]

$$\mathbf{x}_i(t) = \mathbf{x}_i(t-1) + \mathbf{v}_i(t) \tag{1}$$

where $\mathbf{x}_i(t)$ and $\mathbf{x}_i(t-1)$ are the positions vectors of the ith particle at the instants t and $t-1$, respectively, and $\mathbf{v}_i(t)$ is the velocity vector of the particle.

The velocity vector of each particle reflects the individual experience of this particle, and the knowledge of other particles in its neighborhood:

$$\begin{aligned}\mathbf{v}_i(t) = {} & \mathbf{v}_i(t-1) + \varphi_1 \cdot r_1 \cdot (\mathbf{pbest}_i - \mathbf{x}_i(t-1)) \\ & + \varphi_2 \cdot r_2 \cdot (\mathbf{gbest} - \mathbf{x}_i(t-1))\end{aligned} \tag{2}$$

where φ_1 and φ_2 are the individual and the social acceleration constants, respectively, that must meet with the following condition: $\varphi_1 + \varphi_2 \geq 4$ [36], and in this case, they have the same value: $\varphi_1 = \varphi_2 = 2$; r_1 and r_2 are random numbers in the range [0,1]; and $\mathbf{pbest}_i$ and $\mathbf{gbest}$ are the best position vectors found by the *i*th particle and by all the particles, respectively. These parameters reflect the knowledge of the particles.

The vectors $\mathbf{pbest}_i$ and $\mathbf{gbest}$ are evaluated by using a fitness function $J(\mathbf{x})$ that represents the parameter or parameters to be optimized in the reconfiguration problem:

$$\mathbf{x}_i(t) = \mathbf{x}_i(t-1) + \mathbf{v}_i(t) \tag{3}$$

where $P_1,\ P_1,\ \ldots$, represent the parameters to be optimized, and $w_1,\ w_2,\ \ldots$, are the weights assigned to the parts of the fitness function. In this case, the target is to minimize power loss, and so, the optimal particle is the one with the lowest value after evaluating the fitness function.

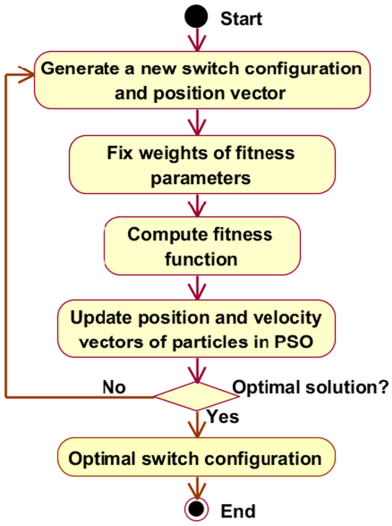

Fig. 1. PSO algorithm activity chart.

In the cases where the combination of switches is not feasible, the fitness function takes on a very high value.

To start the algorithm, an initial position vector is randomly selected, and it is updated in each algorithm iteration. Fig. 1 shows an UML activity chart of the PSO algorithm implemented in this paper. The first step is to generate a new switch configuration and position vector. The second step is to establish the weight of the different parameters of the fitness function. The third step is to compute the fitness function following (3). Then, position and velocity vectors are updated. At this point, if the optimal solution is achieved, the algorithm ends. Otherwise, a new switch configuration and position vector is generated.

III. Use Case

As an application of the reconfiguration algorithm explained in the previous section, in this paper, the optimal control of a meshed power transmission system (HVDC and HVAC mixed network) is designed.

In this section, the objectives of the reconfiguration system and the power transmission grid used are described. Also, short overviews about wind energy generation profiles, circuit breakers, and grid topologies are included.

A. Objectives of the Reconfiguration System

The main objective of the reconfiguration system is to minimize power losses in the transmission system. As mentioned in the previous section, power loss minimization will be achieved by changing the interconnections between the different nodes of the transmission network. Therefore, the reconfiguration system must calculate the best combination of open and closed circuit breakers, in order to minimize the system losses. Two different approaches can be used to achieve this goal, and both are explained in the following sections:

1) Minimize the total losses in the system.
2) Distribute homogenously the losses among all the lines.

1) Minimizing the Total Losses in the System: The target for the reconfiguration algorithm in the first case is the minimization of total losses in the power transmission system. For this, the following steps are conducted:

1) Transmission network data are registered (voltage, current, power, etc.)
2) Power losses in all lines are calculated.
3) The system's total power losses are calculated by adding the losses noted in different lines.
4) The optimization algorithm PSO is executed with the following fitness function:

$$J(\mathbf{x}) = w_1 P_t \tag{4}$$

where

$$P_t = P_{\text{line1}} + P_{\text{line2}} + \cdots + P_{\text{line}N} \tag{5}$$

being $P_{\text{line1}}, \ldots, P_{\text{line}N}$ the power losses in lines 1 to *N*, and P_t the total power losses; and w_1 is the weight of this part of the fitness function, as explained in (3). Note that as in this case there is only one parameter in the fitness function, the weight constant could be eliminated, nevertheless, it has been maintained in (4) to preserve the standard expression.

1) After the algorithm execution, the obtained reconfiguration solution is applied to the transmission network, through the opening or closing of the corresponding circuit breakers.

2) Distribute Homogenously the Losses Among All the Lines: In the second case, the objective was to distribute the losses between all lines in the interconnection system homogenously. This task was achieved following this process (steps 1, 2, and 5 are the same as in the previous case):

1) Transmission network data are registered (voltage, current, power, etc.)
2) Power losses in all lines are calculated.
3) The losses per kilometer are calculated as the relation between losses in a line and its length.
4) The maximum losses per kilometer are minimized by using PSO algorithm.

In this case, the fitness function will be

$$J(\mathbf{x}) = w_1 P_d \tag{6}$$

where

$$P_d = \max\left(\frac{P_{\text{line1}}}{d_1}, \frac{P_{\text{line2}}}{d_2}, \cdots, \frac{P_{\text{line}N}}{d_N}\right) \tag{7}$$

being $d_1, \ldots, d_N$ the length of lines 1 to *N*, $P_{\text{line1}}, \ldots, P_{\text{line}N}$ the power losses in the lines 1 to *N*, and P_d is the maximum value of losses per kilometer.

In both approaches, the losses in each line are calculated as the difference between the power values in its extremes.

B. Energy Generation Profiles

Wind analysis is a very important task that must be carried out as it is one of the criteria that determines where the wind farm will be installed. Other aspects that should be taken into account include geographic restrictions, such as water depth or distance to the shore, the presence of sensible wildlife species,

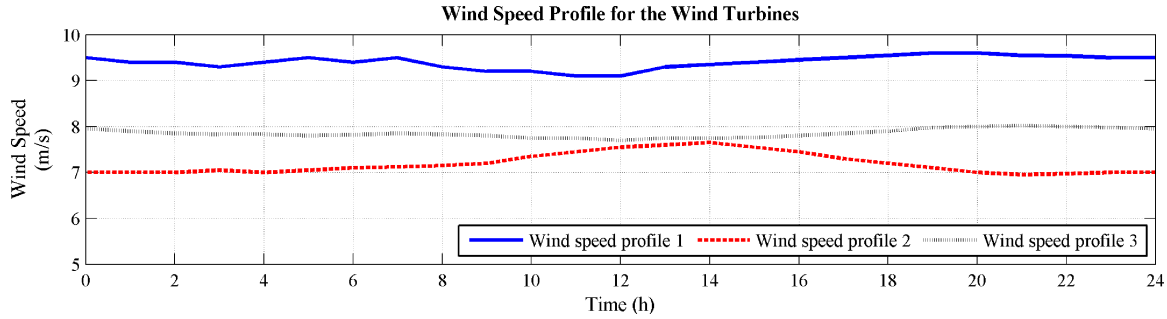

Fig. 2. Generation profiles for the wind turbines.

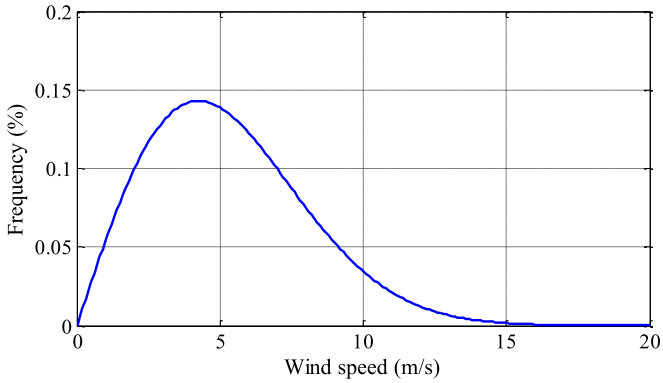

Fig. 3. Weilbull distribution.

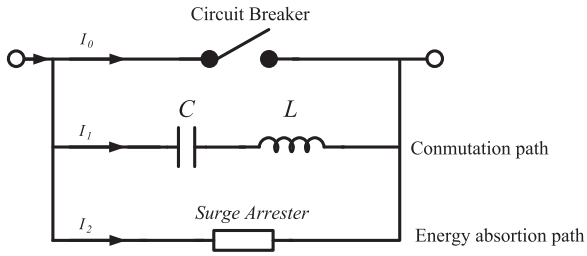

Fig. 4. Mechanical circuit breaker with passive resonator circuit.

or the existence of navigation or air traffic in the zone. With regards to the energy resource in this case, the more the wind is, the higher the amount of electricity generated. Due to this, before a wind farm is built, some studies are carried out in order to find the best areas [37], [38].

Offshore wind farms are usually distributed over very large areas in the sea, therefore, the wind profile in each wind farm may be different. Fig. 2 shows the wind speed profiles used in this paper for the wind farms included in the HVDC test grid, which will be explained in Section III-D. The wind speed profile that corresponds to each wind farm will be specified later.

With the purpose of simulating a real power generation grid, it can be said that the used wind profiles are similar to the most common profiles in offshore wind. The wind speed is usually modeled by using a probability density function. An expression that gives a good fit to wind data is known as the Weibull distribution [39]. The whole wind profile used in this work fit with this statistic function. Fig. 3 shows an example of a Weibull distribution.

C. Circuit Breaker

The circuit breaker is one of the most important elements in the multiterminal HVDC reconfiguration grid. Its function is to open and close the different lines of the grid, in order to change the power flow direction.

There are significant differences between the ac and dc circuit breakers, mainly due to the absence of a natural current zero crossing in the dc systems. Numerous proposals for circuit breakers have been proposed in both papers and patent applications. Nowadays, there are two main types of circuit breaker designed to work in HVDC: electromechanical and solid-state [40].

The electromechanical circuit breakers began to develop in 1980s, when the interest for the HVDC meshed grid increased. During these years, a considerable amount of research and development were conducted [41], [42]. Mechanical dc circuit breakers consist of a conventional ac circuit breaker that has been supplemented by a parallel resonant circuit [43]. The time for current interruption is typically 30–100 ms [44].

Solid-state circuit breakers are the alternatives to electromechanical circuit breakers [45]. The main advantage of these breakers is that their interruption time is very short, just a few milliseconds [46]. This interruption time is only possible by using semiconductor devices. Generally, in solid-state circuit breakers, many IGBTs, IGCTs, or other semiconductor-based switches are connected in series and parallel, in order to support the voltage and current of the system during both normal and fault conditions [47].

In a reconfiguration scenario, in contrast with the fault isolating scenario, the circuit breaker does not need to be extremely fast. In addition, the working current that must be interrupted is the nominal current of the system, that is fairly small compared to the short-circuit current.

According to the previous explanation, the circuit breaker chosen to perform the reconfiguration is the mechanical one with passive resonance circuit. Fig. 4 shows the diagram of the circuit breaker chosen in this case.

During normal operation, the circuit breaker is closed; therefore, the current flows through it while the capacitor is not charged. When the circuit breaker is open, a voltage arc excites the *LC* circuit, generating a current oscillation. This current

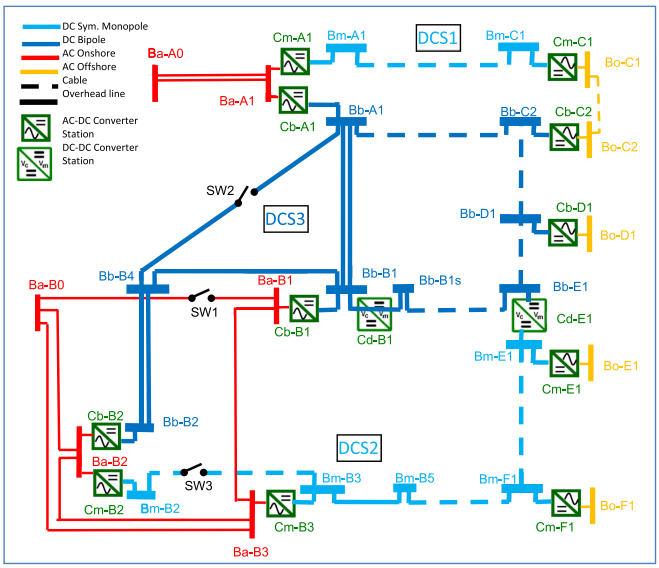

Fig. 5. CIGRE transmission system [32] with the added circuit breakers CB1, CB2, and CB3.

oscillation grows, and thus, creates current zero points in the breaker arc, in order to facilitate the isolation of the circuit. A surge arrester is connected in parallel with the circuit breaker, in order to limit the breaker voltage and absorb the system's energy.

The power losses in an electromechanical circuit breaker are very low, less than 0.001% of the VSC station power losses [47].

D. Interconnection Grid Description

Different topologies can be used to transport the power from wind farms. An extensive study on HVDC topologies is carried out in [49], where the advantages and disadvantages of each topology are shown.

In this paper, the system where the PSO reconfiguration algorithm has been implemented is the test transmission grid described in [32], which is named "CIGRE B4 DC Grid Test System." To test the reconfiguration algorithm in this grid, three circuit breakers have been added to enable the reconfiguration task. Fig. 5 shows the CIGRE transmission system with added switches.

The three circuit breakers added to the CIGRE transmission grid are in one ac line and two dc lines, one of each dc voltage levels. The decision for the breakers' positions has been taken after considering the system's stability. This means that some tests have been done to guarantee that with the breakers in these positions, the system is stable, no matter if the breakers are open or closed.

The CIGRE transmission system is composed by two onshore ac systems (A and B), four offshore ac systems (C, D, E, and F), and the ac and dc connections between them. Onshore systems A and B have points of distributed generation, and also consumption points, meanwhile, offshore systems C, D, and F are wind power plants, and system E is an offshore load. Table I shows the information of the mentioned systems, where the negative values represent power generation and positive values represent load.

TABLE I
ONSHORE AND OFFSHORE SYSTEMS CHARACTERIZATION DATA

	Generation	Load
	Onshore	
A1	−2000 MW	1000 MW
B1	−1000 MW	2200 MW
B2	−1000 MW	2300 MW
B3	−1000 MW	1900 MW
	Offshore	
C1	−500 MW	0 MW
C2	−500 MW	0 MW
D1	−1000 MW	0 MW
E1	0 MW	100 MW
F1	−500 MW	0 MW

TABLE II
POWER TRANSMISSION LINES CHARACTERIZATION DATA

Connected Systems	Type	Voltage (kV)	CB	Num. of lines	Distance (km)	R (Ω/km)	L (mH/km)	C (μF/km)
A0-A1	AC	380	–	2	200	0.0200	0.8532	0.0135
B0-B1	AC	380	CB1	1	200	0.0200	0.8532	0.0135
B0-B2	AC	380	–	1	200	0.0200	0.8532	0.0135
B0-B3	AC	380	–	1	200	0.0200	0.8532	0.0135
B2-B3	AC	380	–	1	200	0.0200	0.8532	0.0135
B1-B3	AC	380	–	1	200	0.0200	0.8532	0.0135
C1-C2	AC	145	–	1	50	0.0843	0.2526	0.1837
A1-B1	DC	400	–	2	400	0.0114	0.9356	0.0123
A1-B4	DC	400	CB2	1	500	0.0114	0.9356	0.0123
A1-C1	DC	200	–	1	200	0.0095	21.110	0.2104
A1-C2	DC	400	–	1	200	0.0095	21.120	0.1906
B1-B4	DC	400	–	1	200	0.0114	0.9356	0.0123
B1-E1	DC	400	–	1	200	0.0095	21.120	0.1906
B2-B3	DC	200	CB3	1	200	0.0095	21.110	0.2104
B2-B4	DC	400	–	2	300	0.0114	0.9356	0.0123
B3-B5	DC	200	–	1	100	0.0133	0.8273	0.0139
B5-F1	DC	200	–	1	100	0.0095	21.110	0.2104
C2-D1	DC	400	–	1	300	0.0095	21.120	0.1906
D1-E1	DC	400	–	1	200	0.0095	21.120	0.1906
E1-F1	DC	200	–	1	200	0.0095	21.110	0.2104

Some of the interconnections between the onshore and offshore systems are in dc, and others are in ac, and in each type, there are lines for two different voltages. The characteristics of all these lines in the system are summarized in Table II.

Although in the CIGRE system only the nominal generated power for the wind farms appears, in this paper, the power generation profile shown in Fig. 6 has been used to simulate the operation of wind power plants. These profiles have been obtained from the speed profiles shown in Fig. 2: The wind speed profile 1 is used for wind farms C1 and C2; profile 2 is used for D1, and wind speed profile 3 is used for F1.

As three circuit breakers have been added to the CIGRE Grid Test System, there are eight (that are 2^3) different combinations, and, in this case, all of them are feasible because the positioning process of the breakers has been done carefully. The default

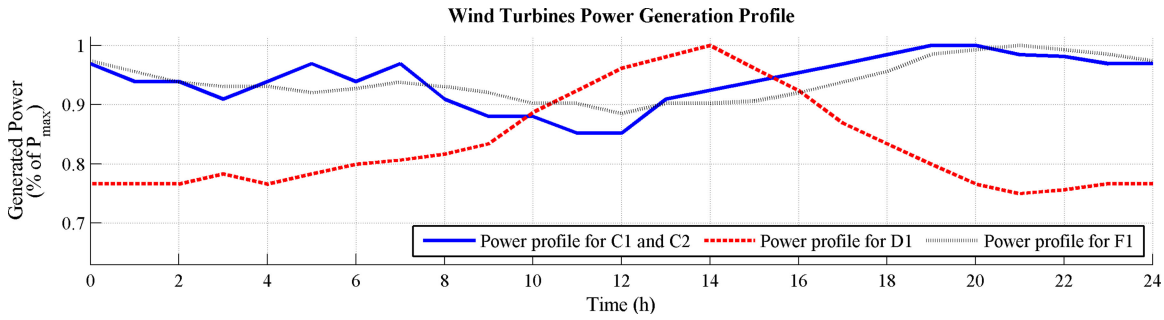

Fig. 6. Wind farms power generation profile.

TABLE III
RECONFIGURATION SOLUTIONS FOR THE USED GRID

Combination Id.	CB1 (AC, 380 kV)	CB2 (DC, 400 kV)	CB3 (DC, 200 kV)
1	0	0	0
2	0	0	1
3	0	1	0
4	0	1	1
5	1	0	0
6	1	0	1
7	1	1	0
8*	1	1	1

*The default configuration for this grid is number 8: all the circuit breakers closed.

configuration for this grid is with all the circuit breakers closed. These configurations are shown in Table III.

The wind farms can also be disconnected from the transmission system due to a maintenance task, or in case of no wind. In those cases, the power generated by the other wind farms are redistributed by using the available lines. This produces power flows that must be controlled by using the proposed algorithm.

IV. SIMULATION RESULTS

The results shown in this section have been obtained from the abovedescribed CIGRE HVDC grid simulation model. The system model has been built with Matlab–Simulink software, following the characteristics of the test grid explained in [32].

According to the fitness functions explained in Section III-A, the data of the power losses in all the lines of the grid are registered, and then used to execute the reconfiguration algorithm.

Some tests have been done to check the algorithm's effectiveness. These tests have been made under the following operation conditions:

1) Normal operation (all wind farms connected).
2) Wind farm F1 disconnected.

To simulate the hourly operation of the reconfiguration algorithm, the PSO algorithm has been executed 24 times with the corresponding power generation profile data, in order to obtain the best reconfiguration solution for each condition. Therefore, the tests have been made once an hour over a day, according to the mentioned tests, and also following both approaches explained in Section III-A. Fig. 7 shows an example of the movement evolution for some of the particles involved in the PSO execution at 8 AM, especially in the case of approach 1. Note that for clarity purposes, only the movements of 30 of the 300 particles have been represented in that figure. In Fig. 7, it can be seen how the particles start their movements in a random position, and iteration after iteration, they meet in the optimal solution (in the specific case of Fig. 7, the optimal solution is configuration 4).

Figs. 8 and 9 show the reconfiguration results after applying the PSO algorithm to the HVDC connection system under the above conditions for normal operation, and having the wind farm F1 disconnected, respectively. It can be seen that the results are different, depending on the operation conditions and on the approach used to solve the reconfiguration problem.

In those figures, it can be seen that the best reconfiguration solution in the mentioned conditions is not always the default configuration. This means, applying the reconfiguration algorithm improves the system behavior, by reducing the power losses.

In order to better illustrate the effects of reducing the total losses and the maximum losses for the length unit, Figs. 10 and 11 compare the total losses and the maximum loss per length unit by using the reconfiguration algorithm and also in the default configuration. It can be seen that a reduction in the total losses and in the maximum loss per length unit is achieved for those cases where the best configuration is different from the default one.

In order to quantify the losses reduction illustrated in Figs. 10 and 11, the normalized root mean square error (NRMSE) can be calculated as

$$\text{NRMSE} = \sqrt{\frac{1}{N}\sum_{h=1}^{N}\left(\frac{P_{\text{default}_h} - P_{\text{reconfiguration}_h}}{P_{\text{default}_h}}\right)^2} \cdot 100\,(\%) \quad (8)$$

where P_{default} represents the losses with the default configuration, and $P_{\text{reconfiguration}}$ are the losses with the reconfiguration solution obtained for each case. As in this case the reconfiguration process has been simulated for the periods of an hour over a day, N is 24. The NRMSE obtained with the simulation results is 19.3% for the total losses reduction approach, what means that the total losses could be reduced by 19.3%. In the losses distribution approach, the NRMSE is 18.7%. In this case, it represents the way in which the losses could be better distributed among all the lines, and the maximum loss per length of unit could be reduced in 18.7%, increasing, in this way, the life time of the lines.

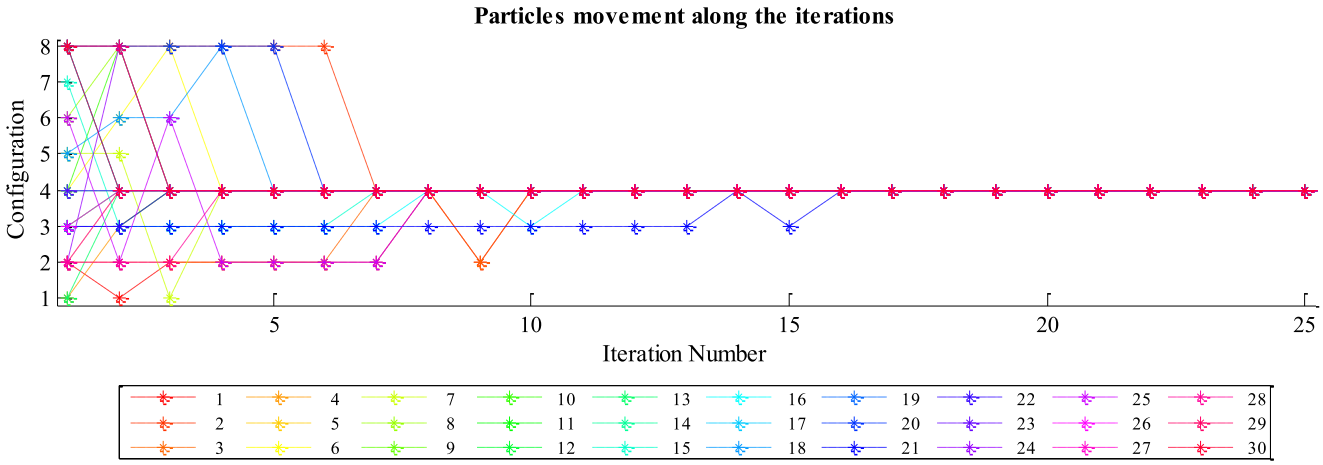

Fig. 7. Example of the movement of thirty particles along the iterations, for the case of executing the PSO algorithm at 8 A.M. in approach 1.

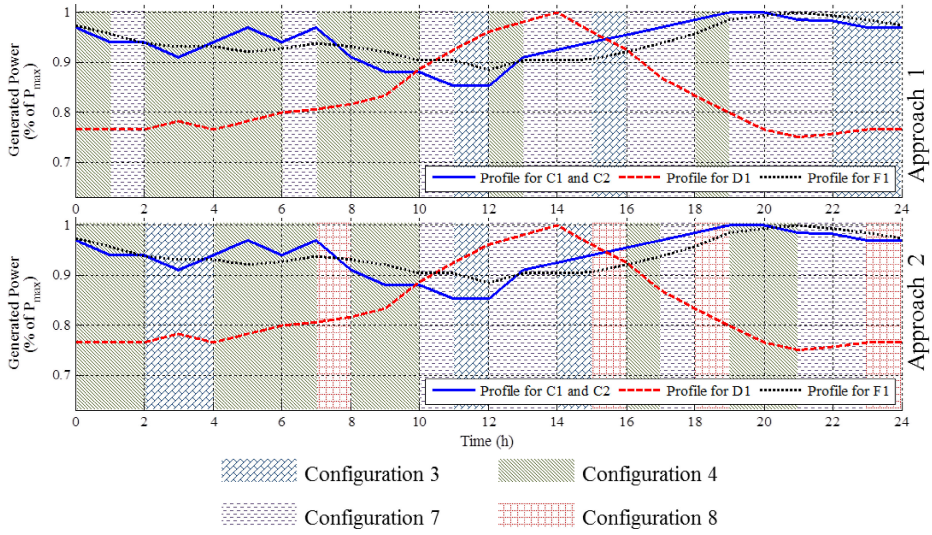

Fig. 8. Best reconfiguration solution along a day in case of normal operation for both approaches: Minimizing the total losses, and minimizing the total losses per length unit.

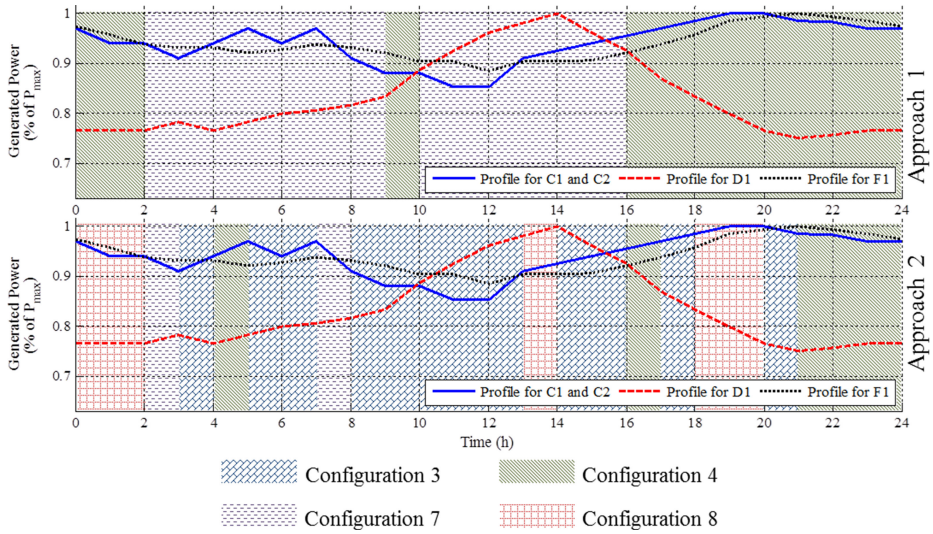

Fig. 9. Best reconfiguration solution along a day, in case of having wind farm F1 disconnected for both approaches: Minimizing the total losses, and minimizing the total losses per length unit.

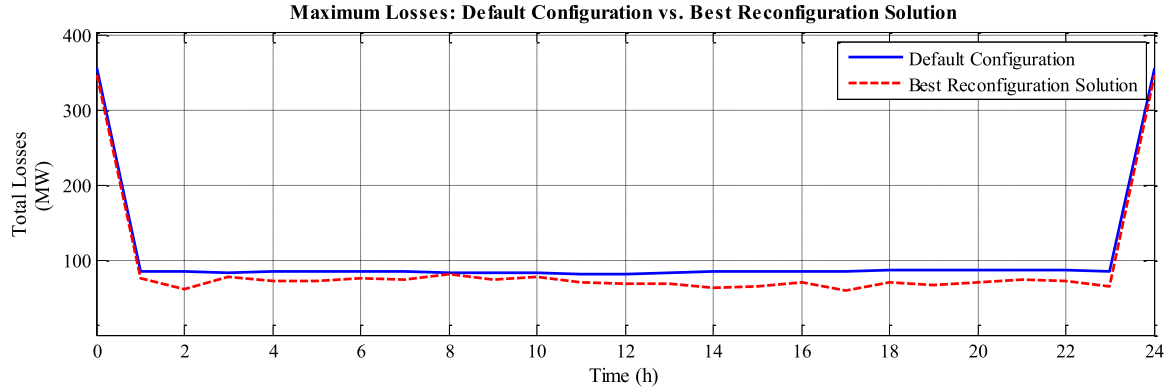

Fig. 10. Total losses with the default configuration (blue line) and using the reconfiguration algorithm (dashed red line).

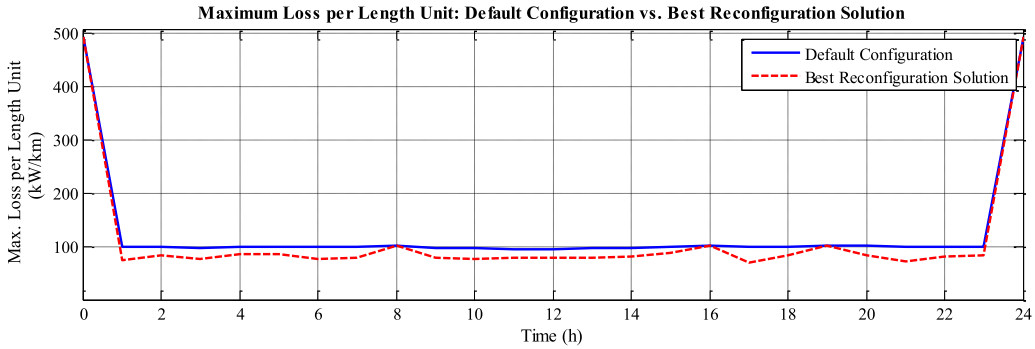

Fig. 11. Maximum loss per length unit in the default configuration (blue line), and using the reconfiguration algorithm (dashed red line).

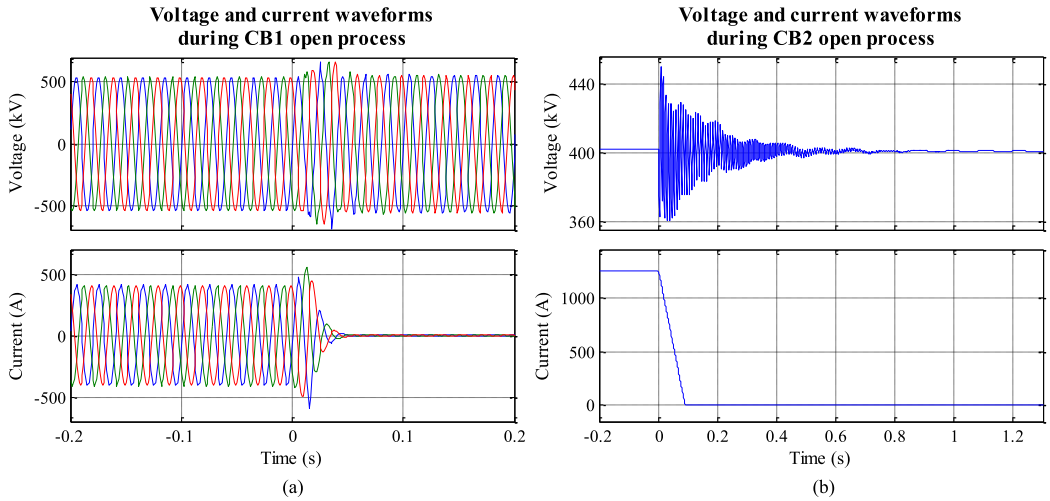

Fig. 12. (a) Voltage and current waveforms during the open process of CB1 (ac circuit breaker), and (b) CB2 (dc circuit breaker).

In order to illustrate the operation of the circuit breakers in the HVDC grid, in Fig. 12, the worst-case voltage and current waveforms, corresponding with CB1 and CB2, are represented. Fig. 12(a) and (b) represents, respectively, the open process of an AC circuit breaker (CB1) and a DC circuit breaker (CB2), where the instant 0 indicates the moment when the CB is opened. As it can be observed, the times of voltage stabilization and current interruption are lower in the case of ac circuit breaker, because each system has different dynamics.

V. Conclusion

The development of multiterminal HVDC transmission grids represents a breakthrough in the efficiently and reliability of energy distribution over long distances. Large plans to build offshore wind farms have increased the development in this kind of transmission systems.

This paper proposes the use of a reconfiguration algorithm in a HVDC meshed grid, as a complement to those control techniques that are generally used in this kind of grids.

In this paper, a reconfiguration algorithm has been implemented in a complex HVDC power transmission system, in order to reduce power losses. Two different approaches have been used: one to minimize the total losses and another to distribute those losses.

After testing the reconfiguration algorithm in the described grid, it is proved that the system is able to adapt to the changing conditions in order to minimize or distribute the losses. Moreover, the simulation results shown above prove that the proposed reconfiguration algorithm, based on PSO algorithm, is very suitable for this kind of applications.

The reconfiguration algorithm has shown that as the energy generation changes due to wind changes, the grid topology must be changed as well, in order to achieve maximum efficiency.

As future work, a comparison between the results obtained by using the PSO reconfiguration algorithm, and the results obtained from varying the parameters in the VSC control, will be carried out. Moreover, the PSO-based reconfiguration algorithm could also be used to optimize the parameters of the VSC control.

REFERENCES

[1] G. P. Beretta, "World energy consumption and resources: an outlook for the rest of the century," *Int. J. Environ. Technol. Manage.*, vol. 7, nos. 1/2, pp. 99–112, 2007.

[2] European Commission, "World energy, technology and climate policy outlook," 2003.

[3] J. P. Hansen, P. A. Narbel, and D. L. Aksnes, "Limits to growth in the renewable energy sector," *Renewable Sustain. Energy Rev.*, vol. 70, pp. 769–774, 2017.

[4] W. Crijns-Graus, "Renewable energy: Past trends and future growth in 2 degrees scenarios," *Energy Procedia*, vol. 100, pp. 14–21, 2016.

[5] National Renewable Research Laboratory, "Hawaii solar integration study: Executive summary," 2013.

[6] S. Wang, S. Wang, and P. Smith, "Quantifying impacts of onshore wind farms on ecosystem services at local and global scales," *Renewable Sustain. Energy Rev.*, vol. 52, pp. 1424–1428, Dec. 2015.

[7] P. Higgins and A. Foley, "The evolution of offshore wind power in the United Kingdom," *Renewable Sustain. Energy Rev.*, vol. 37, pp. 599–612, Sep. 2014.

[8] N. M. Kirby, M. J. Luckett, L. Xu, and W. Siepmann, "HVDC transmission for large offshore windfarms," in *Proc. 7th Int. Conf. AC-DC Power Transmiss.* (Conf. Publ. No. 485), 2001, pp. 162–168.

[9] P. Bresesti, W. L. Kling, R. L. Hendriks, and R. Vailati, "HVDC connection of offshore wind farms to the transmission system," *IEEE Trans. Energy Convers.*, vol. 22, no. 1, pp. 37–43, Mar. 2007.

[10] N. M. Kirby, L. Xu, M. Luckett, and W. Siepmann, "HVDC transmission for large offshore wind farms," *Power Eng. J.*, vol. 16, no. 3, pp. 135–141, Jun. 2002.

[11] L. Xu, B. W. Williams, and L. Yao, "Multi-terminal DC transmission systems for connecting large offshore wind farms," in *Proc. IEEE Power Energy Soc. Gen. Meet.-Convers. Del. Electr. Energy 21st Century*, 2008, pp. 1–7.

[12] J. Zhu and C. Booth, "Future multi-terminal HVDC transmission systems using voltage source converters," in *Proc. IEEE 45th Int. Univers. Power Eng. Conf.*, 2010, pp. 1–6.

[13] D. Jovcic and B. T. Ooi, "Developing DC transmission networks using DC transformers," *IEEE Trans. Power Del.*, vol. 25, no. 4, pp. 2535–2543, Oct. 2010.

[14] F. D. Bianchi and O. Gomis-Bellmunt, "Droop control design for multi-terminal VSC- HVDC grids based on LMI optimization," in *Proc. 50th IEEE Conf. Decis. Control Eur. Control conf.*, 2011, pp. 4823–4828.

[15] L. Jun, T. Jing, O. Gomis-Bellmunt, J. Ekanayake, and N. Jenkins, "Operation and control of multiterminal HVDC transmission for offshore wind farms," *IEEE Trans. Power Del.*, vol. 26, no. 4, pp. 2596–2604, Oct. 2011.

[16] V. Nasirian, S. Moayedi, A. Davoudi, and F. L. Lewis, "Distributed cooperative control of DC microgrids," *IEEE Trans. Power Electron.*, vol. 30, no. 4, pp. 2288–2303, Apr. 2015.

[17] M. Aragüés-Peñalba, A. Egea-Àlvarez, O. Gomis-Bellmunt, and A. Sumper, "Optimum voltage control for loss minimization in HVDC multi-terminal transmission systems for large offshore wind farms," *Elect. Power Syst. Res.*, vol. 89, pp. 54–63, Aug. 2012.

[18] G. Daelemans, K. Srivastava, M. Reza, S. Cole, and R. Belmans, "Minimization of steady-state losses in meshed networks using VSC HVDC," in *Proc. IEEE Power Energy Soc. Gen. Meet.*, Calgary, AB, USA, 2009, pp. 1–5

[19] J. Cao, W. Du, H. F. Wang, and S. Q. Bu, "Minimization of transmission loss in meshed AC/DC grids with VSC-MTDC networks," *IEEE Trans. Power Syst.*, vol. 28, no. 3, pp. 3047–3055, Aug. 2013.

[20] J. Olamei, T. Niknam, A. Arefi, and A. H. Mazinan, "A novel hybrid evolutionary algorithm based on ACO and SA for distribution feeder reconfiguration with regard to DGs," in *Proc. GCC Conf. Exhib.*, 2011, pp. 259–262.

[21] F. Scenna, D. Anaut, L. I. Passoni, and G. J. Meschino, "Reconfiguration of electrical networks by an ant colony optimization algorithm," *IEEE Latin Amer. Trans.*, vol. 11, no. 1, pp. 538–44, Feb. 2013.

[22] H. D. de Macedo Braz and B. A. de Souza, "Distribution network reconfiguration using genetic algorithms with sequential encoding: Subtractive and additive approaches," *IEEE Trans. Power Syst.*, vol. 26, no. 2, pp. 582–93, May 2011.

[23] B. Radha, R. T. F. King, and H. C. S. Rughooputh, "A modified genetic algorithm for optimal electrical distribution network reconfiguration," in *Proc. IEEE Congr. Evolutionary Comput.*, 2003, pp. 1472–1479.

[24] A. Zidan and E. F. El-Saadany, "Distribution system reconfiguration for energy loss reduction considering the variability of load and local renewable generation," *Energy*, vol. 59, pp. 698–707, Sep. 2013.

[25] N. Gupta, A. Swarnkar, and K. R. Niazi, "Distribution network reconfiguration for power quality and reliability improvement using genetic algorithms," *Int. J. Elect. Power Energy Syst.*, vol. 54, pp. 664–671, Jan. 2014.

[26] A. C. B. Delbem, A. C. de Carvalho, and N. G. Bretas, "Main chain representation for evolutionary algorithms applied to distribution system reconfiguration," *IEEE Trans. Power Syst.*, vol. 20, no. 1, pp. 425–436, Feb. 2005.

[27] A. Mendes, N. Boland, P. Guiney, and C. Riveros, "Switch and tap-changer reconfiguration of distribution networks using evolutionary algorithms," *IEEE Trans. Power Syst.*, vol. 28, no. 1, pp. 85–92, Feb. 2013.

[28] F. Y. Hsu and M. S. Tsai, "A multi-objective evolution programming method for feeder reconfiguration of power distribution system," in *Proc. IEEE 13th Int. Conf. Intell. Syst. Appl. Power Syst.*, 2005, pp. 55–60.

[29] R. Syahputra, I. Robandi, and M. Ashari, "Reconfiguration of distribution network with DG using fuzzy multi-objective method," in *Proc. Int. Conf. Innov. Manage. Technol. Res.*, 2012, pp. 316–321.

[30] B. Amanulla, S. Chakrabarti, and S. N. Singh, "Reconfiguration of power distribution systems considering reliability and power loss," *IEEE Trans. Power Del.*, vol. 27, no. 2, pp. 918–926, Apr. 2012.

[31] J. Olamei, G. Gharehpetian, and T. Niknam, "An approach based on particle swarm optimization for distribution feeder reconfiguration considering distributed generators," in *Proc. IEEE Power Syst. Conf.: Adv. Metering, Protec., Control, Commun., Distrib. Resources*, 2007, pp. 326–330.

[32] T. K. Vrana, Y. Yang, D. Jovcic, S. Dennetière, J. Jardini, and H. Saad, "The CIGRE B4 DC grid test system," *Electra*, vol. 270, pp. 10–19, 2013.

[33] K. Rouzbehi, A. Miranian, A. Luna, and P. Rodriguez, "DC voltage control and power sharing in multiterminal DC grids based on optimal DC power flow and voltage-droop strategy," *IEEE J. Emerging Sel. Topics Power Electron.*, vol. 2, no. 4, pp. 1171–1180, Dec. 2014.

[34] K. Rouzbehi, A. Miranian, J. I. Candela, A. Luna, and P. Rodriguez, "A generalized voltage droop strategy for control of multiterminal DC grids," *IEEE Trans. Ind. Appl.*, vol. 51, no. 1, pp. 607–618, Jan./Feb. 2015.

[35] D. E. Olivares, J. D. Lara, C. A. Cañizares, and M. Kazerani, "Stochastic-predictive energy management system for isolated microgrids," *IEEE Trans. Smart Grid*, vol. 6, no. 6, pp. 2681–2693, Nov. 2015.

[36] Y. del Valle, G. K. Venayagamoorthy, S. Mohagheghi, J. C. Hernandez, and R. G. Harley, "Particle swarm optimization: Basic concepts, variants and applications in power systems," *IEEE Trans. Evolutionary Comput.*, vol. 12, no. 2, pp. 171–195, Apr.l 2008.

[37] D. C. Hill, D. McMillan, K. R. W. Bell, and D. Infield, "Application of auto-regressive models to U. K. wind speed data for power system impact studies," *IEEE Trans. Sustain. Energy*, vol. 3, no. 1, pp. 134–141, Jan. 2012.
[38] N. Fichaux, T. Poglio, and T. Ranchin, "Mapping offshore wind resources: Synergetic potential of SAR and scatterometer data," *IEEE J. Ocean. Eng.*, vol. 30, no. 3, pp. 516–525, Jul. 2005.
[39] T. H. Yeh and L. Wang, "A study on generator capacity for wind turbines under various tower heights and rated wind speeds using Weibull distribution," *IEEE Trans. Energy Convers.*, vol. 23, no. 2, pp. 592–602, Jun. 2008.
[40] C. M. Franck, "HVDC circuit breakers: A review identifying future research needs," *IEEE Trans. Power Del.*, vol. 26, no. 2, pp. 998–1007, Apr. 2011.
[41] W. Pucher, P. Joss, B. Koetzold, T. Lee, and V. Zajic, "HVDC switching devices and arrangements," *Electra*, no. 18, pp. 9–65, Jul. 1971.
[42] J. J. Vithayathil, A. L. Courts, W. G. Peterson, N. G. Hingorani, S. L. Nilsson, and J. W. Porter, "HVDC circuit breaker development and field tests," *IEEE Power Eng. Rev.*, vol. PER-5, no. 10, pp. 29–30, Oct. 1985.
[43] T. Senda, T. Tamagawa, K. Higuchi, T. Horiuchi, and S. Yanabu, "Development of HVDC circuit breaker based on hybrid interruption scheme," *IEEE Trans. Power Appl. Syst.*, vol. PAS-103, no. 3, pp. 545–552, Mar. 1984.
[44] B. Pauli, G. Mauthe, E. Ruoss, G. Ecklin, J. Porter, and J. Vithayathil, "Development of a high current HVDC circuit breaker with fast fault clearing capability," *IEEE Trans. Power Del.*, vol. 3, no. 4, pp. 2072–2080, Oct. 1988.
[45] C. M. Franck, "HVDC circuit breakers: A review identifying future research needs," *IEEE Trans. Power Del.*, vol. 26, no. 2, pp. 998–1007, Apr. 2011.
[46] K. Sano and M. Takasaki, "A surgeless solid-state DC circuit breaker for voltage-source-converter-based HVDC systems," *IEEE Trans. Ind. Appl.*, vol. 50, no. 4, pp. 2690–2699, Jul./Aug. 2014.
[47] A. Mokhberdoran, A. Carvalho, H. Leite, and N. Silva, "A review on HVDC circuit breakers," in *Proc. 3rd Renewable Power Gen. Conf.*, Sept. 2014, pp. 1–6.
[48] T. Ackermann, *Wind Power in Power Systems*. London, U.K.: Wiley, 2012, Appendix 7.
[49] O. Gomis-Bellmunt, J. Liang, J. Ekanayake, R. King, and N. Jenkins, "Topologies of multiterminal HVDC-VSC transmission for large offshore wind farms," in *Elect. Power Syst. Res.*, vol. 81, no. 2, pp. 271–281, Feb. 2011.

Inés Sanz received the B.S. degree in industrial engineering from the Technical University of Madrid, Spain, in 2012, and the M.S. degree in industrial processes automation from the University of Alcalá, Spain, in 2012.

She is member of the Group of Electronic Engineering Applied to Renewable Energy Systems in University of Alcalá, Spain, where she is working toward the Ph. D. degree. Her fields of interest include power electronics systems and power converters.

Miguel Moranchel received the B.S. degree in electronic engineering from University of Alcalá, Alcalá de Henares, Spain, in 2010, and the M.S. degree in industrial processes automation from the University of Alcalá, Spain, in 2012. He is currently working toward the Ph.D. degree in the Department of Electronics, University of Alcalá, where he is a member of the research group "Electronics Engineering Applied to the Renewable Energies".

His research areas include power electronic systems and digital systems.

Javier Moriano (S'16) was born in Alcalá de Henares, Spain, in 1992. He received the B. S. degree in industrial electronics and automation engineering and the M. S. degree in industrial engineering from the University of Alcalá (Spain) in 2014 and 2016, respectively. He is currently pursuing the Ph.D. degree in electronics engineering from the university of Alcalá (Spain) and he is member of the research group "Electronics Engineering Applied to the Renewable Energies."

His current research interests include multifrequency control, renewable energy integration and distributed generation.

Francisco Javier Rodríguez (S'99–M'00) received the B.Sc. degree in technical telecommunication engineering from the University of Alcalá, Alcalá de Henares, Spain, in 1985, the M.Sc. degree in telecommunication from the Technical University of Madrid, Madrid, Spain, in 1990, and the Ph.D. degree in electronics engineering from the University of Alcalá in 1997.

He worked in the private electronic industry for two years. Since 1986, he has been a Lecturer with the Department of Electronics, University of Alcalá, where he is a Professor. He is the author of more than 142 refereed publications in international journals, book chapters, and conference proceedings. Also, he has directed more than 45 investigation projects funded by public institutions and private industry. His research interests include the areas of control electronics, real-time processing, and embedded systems applied to power electronic systems.

Susel Fernandez received the B.S. and M.S. degrees in computer science from The University of Oriente, Cuba, and the Ph.D. degree from the University of Alcala, Alcalá de Henares, Spain, in 2013.

She is currently working as an Assistant Professor at the Nagoya Institute of Technology, Nagoya, Japan. Her main research interest focuses on applications of artificial intelligence, multiagent systems, and knowledge-based systems, especially ontologies.